Northumbria Research Link

Citation: Lu, Shun, Hummel, Matthew, Gu, Zhengrong, Wang, Yucheng, KeWang, Keliang, Pathak, Rajesh, Zhou, Yue Zhou, Jia, Hongxing, Qi, Xueqiang, Xu, Bin and Liu, Xiaoteng (2021) Highly efficient urea oxidation via nesting nano nickel oxide in eggshell membrane-derived carbon. ACS Sustainable Chemistry and Engineering, 9 (4). pp. 1703-1713. ISSN 2168-0485

Published by: American Chemical Society

URL: https://doi.org/10.1021/acssuschemeng.0c07614 <https://doi.org/10.1021/acssuschemeng.0c07614>

This version was downloaded from Northumbria Research Link: http://nrl.northumbria.ac.uk/id/eprint/45146/

Northumbria University has developed Northumbria Research Link (NRL) to enable users to access the University's research output. Copyright © and moral rights for items on NRL are retained by the individual author(s) and/or other copyright owners. Single copies of full items can be reproduced, displayed or performed, and given to third parties in any format or medium for personal research or study, educational, or not-for-profit purposes without prior permission or charge, provided the authors, title and full bibliographic details are given, as well as a hyperlink and/or URL to the original metadata page. The content must not be changed in any way. Full items must not be sold commercially in any format or medium without formal permission of the copyright holder. The full policy is available online: http://nrl.northumbria.ac.uk/policies.html

This document may differ from the final, published version of the research and has been made available online in accordance with publisher policies. To read and/or cite from the published version of the research, please visit the publisher's website (a subscription may be required.)

Northumbria University NEWCASTLE

University Library

Highly efficient urea oxidation via nesting nano nickel oxide in eggshell membrane-derived carbon

Shun Lu[ab], Matthew Hummel[a], Zhengrong Gu[a,*], Yucheng Wang[b], Keliang Wang[c], Rajesh Pathak[d], Yue Zhou[d], Hongxing Jia[a], Xueqiang Qi[e,*], Xianhui Zhao[f], Ben Bin Xu[b], Xiaoteng Liu[b,*]

a Department of Agricultural and Biosystems Engineering, South Dakota State University, Brookings, SD, 57007, USA

b Department of Mechanical & Construction Engineering, Faculty of Engineering and Environment, Northumbria University, Newcastle upon Tyne, NE1 8ST, UK

c Department of Electrical Engineering and Computer Engineering & Department of Chemical Engineering and Materials Science, Michigan State University, East Lansing, MI, 48824, USA

d Department of Electrical Engineering and Computer Science, South Dakota State University, Brookings, SD, 57007, USA

e College of Chemistry and Chemical Engineering, Chongqing University of Technology, Chongqing, 400054, China

f Manufacturing Science Division, Oak Ridge National Laboratory, 1 Bethel Valley Road, Oak Ridge, Tennessee, 37831, USA

[*] Corresponding authors: zhengrong.gu@sdstate.edu (Z. Gu), xqqi@cqut.edu.cn (X. Qi), Terence.liu@northumbria.ac.uk (X. Liu)

Abstract

Here, we reported a strategy of using an eggshell membrane to produce hierarchically porous carbon as a low-cost substrate for synthesizing nano nickel oxide catalyst (C@NiO), which can effectively turn biowaste - urea into energy through an electrochemical approach. The interwoven carbon networks within NiO led to highly efficient urea oxidation due to the strong synergistic effect. The as-prepared electrode only needed 1.36 V *versus* reversible hydrogen electrode to realize high efficiency of 10 mA cm^{-2} in 1.0 M KOH with 0.33 M urea and delivered an even higher current density of 25 mA cm^{-2} at 1.46 V, which is smaller than that of the porous carbon and commercial Pt/C catalyst. Benefiting from theoretical calculations, Ni(III) active species and the porous carbon further enabled the electrocatalyst to effectively inhibit the "CO_2 poisoning" of electrocatalysts, as well as ensuring its superior performance for urea oxidation.

Keywords: nickel oxide; eggshell membrane; porous carbon substrate; urea oxidation; density functional theory.

Introduction

In recent years, there has been a fast-growing trend in developing urea ($CO(NH_2)_2$) as a substitute H_2 carrier in energy conversion due to its high energy density, nontoxicity, stability and non-flammability.[1] Urea, a byproduct in the metabolism of proteins and a frequent contaminant in wastewater, is an abundant compound that has demonstrated favorable characteristics as a hydrogen-rich fuel source with 6.7 *wt.*% in gravimetric hydrogen content.[1-4] Also, there is 2-2.5 *wt.*% urea from mammal urine, therefore, 0.5 million tons of additional fuels will be produced per year just from human urine (240 million tons each year).[5-8] Electrochemical oxidation has been recognized as an efficient strategy for urea conversion and wastewater remediation.[9-11] Thus, the chemical energy harvested from urea/urine can be converted to electricity *via* urea oxidation reaction (UOR).[12-14] Moreover, the removal of urea from water is a priority for improving drinking water quality and presents an opportunity for UOR.[15] However, the transition of UOR from theory and laboratory experiments to real-world applications is largely limited by the conversion efficiency, catalyst cost and the feasibility of wide-spread usage.[16]

Primarily, the electrooxidation of urea has relied on cost-prohibitive rare metals such as ruthenium, platinum, tantalum, or iridium for urea catalysis.[14, 17] Recent studies implementing common transition metals and their oxides, particularly nickel, have found similar success while having much lower material costs.[18-20] For instance, Luo et al. prepared ultrathin and porous nickel hydroxide nanosheets for efficient UOR, and found that 1.82 V (*vs.* RHE, Reversible Hydrogen Electrode) was needed to achieve a large current density of 298 mA cm^{-2}.[21] Qiao et al. reported a two-dimensional nickel-based metal-organic framework (2D Ni-MOF) nanosheets by coordinating nickel ions and benzenedicarboxylic acid. The electrochemical results showed better UOR performance and smaller overpotential compared to $Ni(OH)_2$ and the commercial Pt/C.[13]

Similarly, Ma et al. investigated Ni-MOF with different morphologies such as, nanowires, neurons, and urchins, and found that the Ni-MOF nanowires requires ~0.8 V (*vs.* Ag/AgCl) to obtain a current density of 160 mA cm^{-2}.[22] Thus, based on the previous studies, the nickel-based materials' electrocatalytic behavior is well understood, making them ideal candidates for UOR.[23, 24] However, there is still a sluggish kinetics of UOR at the anodic area owing to the multi-electron transfer and multiple gas-adsorption/desorption procedures.[23-27] To address this key issue, the coordination of high surface area and, conductive materials are considered beneficial.[28-30] Expanding the electrochemically active surface area. The bio-derived carbons doped nickel can provide the electrochemically active high surface area and conductivity in the material selection, resulting in efficient substrates.[31] Innovations with UOR from organic and bio-derived compounds have yielded substantial improvements in energy production efficiency.[32, 33]

Biomass-derived carbon materials have been increasingly implemented in electrochemical energy conversion and detection owing to their low-price, porous structure and high conductivity.[34] Hierarchical porous activated carbons are favored in particular due to their variety in pore size and volume, the potential for modification, and synthesis from waste biomaterials.[35, 36] One promising material that has demonstrated notable electrochemical properties is the eggshell membrane (ESM). ESM is a thin, protein-based membrane functioning as a gas-exchange interface for the embryo within the egg to the outside world via its abundant micro- and nano-sized pores.[37] Aside from the traditional methods of waste management, ESM has been used in the production of clean energy where it replaces coal, oil or natural gases to generate electricity through fuel cell devices. ESM collected from waste eggshells has demonstrated excellent electrochemical behavior on its own in energy storage and conversion [38, 39] as well an ability to be infused with different transition metal oxides for sensing purposes.[40, 41]

In this work, we reported a low-cost UOR electrocatalyst (C@NiO), composed of nickel oxide nanoparticles anchored on the porous carbon derived from the biowaste eggshell membrane *via* hydrothermal synthesis and pyrolysis strategy. Benefiting from the strong synergistic effect between nickel oxide and the porous carbon, the as-prepared electrode only needs 1.36 V *versus* RHE to realize 10 mA cm^{-2} in 1.0 M alkali solution containing 0.33 M urea, and delivers 25 mA cm^{-2} at 1.46 V. In addition, in the viewpoint of the theoretical calculations, its intermediate (C@NiOOH), which formed from C@NiO in alkaline solution, made this electrocatalyst possessing the ability to effectively hinder "CO_2 poisoning", as well as ensuring its superior performance for UOR. This work also presented the low-cost urea oxidation electrocatalyst design with the porous structure to solve the previous problems we described (source and cost) and promote the catalyst's potential application in energy conversion based on the concept of "trash to treasure".

Experimental

Preparation of the porous C@NiO nanocomposites

Before obtaining C@NiO nanocomposites from the biowaste eggshell membrane, the ESM received pre-treatments to remove the left egg white and other organic chemicals. C@NiO nanocomposites were prepared through a smart approach that the eggshell was not only employed as a reactor, but also the eggshell membrane as a filter membrane here, as presented in **Fig. 1**. First, the eggshell filled with $Ni(NO_3)_2$ aqueous solution was transferred into a beaker with urea, then kept at 70 ℃ for 6 h. In this process, $Ni(OH)_2$ was synthesized on the interface of the eggshell membrane as OH^- ions (outside of ESM) were reacted with Ni^{2+} ions (inside of ESM). Then, the eggshell membrane was stripped from the eggshell reactor by tweezers after the reaction system was naturally cooled down. The stripped ESM was washed thoroughly with deionized water.

Completely, black powder was received after calcination at 500 ℃ for two hours in N_2 environment. The calcined black powder with a metallic color was washed and collected for further characterizations.

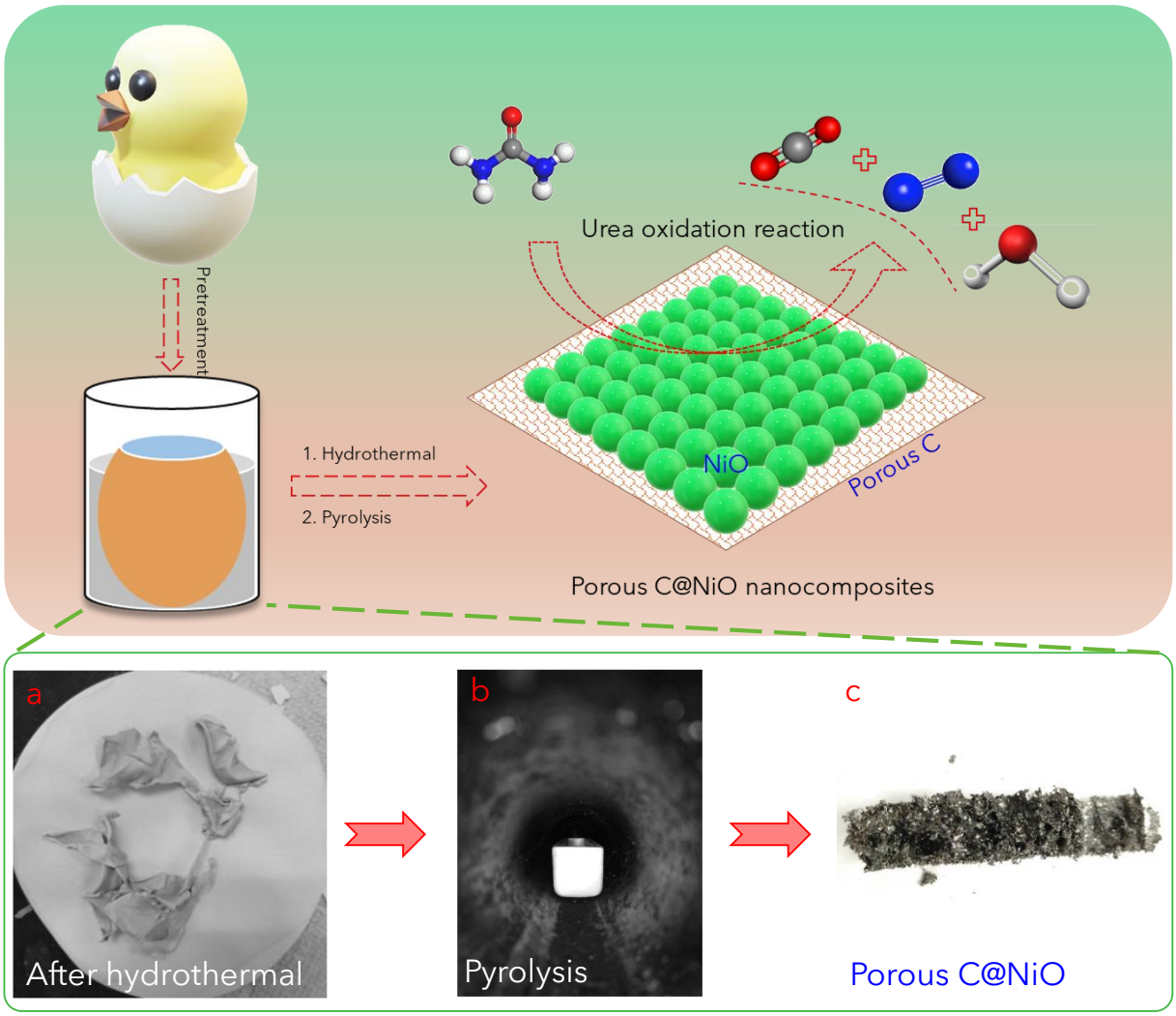

Figure 1. Scheme of the formulation process of the porous C@NiO nanocomposites: (a) dried NiO/ESM after the hydrothermal process, (b) pyrolysis treatment, and (c) final product after the pyrolysis.

Physical characterizations

The scanning electron microscopy (SEM) and transmission electron microscopy (TEM) were both employed to observe the as-prepared samples' morphological information, equipped

with high-resolution TEM (HRTEM) and select area electron diffraction (SAED). Scanning transmission electron microscopy energy dispersive X-ray (STEM-EDX) spectroscopy was employed for analyzing the elements' distribution. The pyrolysis process was investigated to indicate the synthesis of C@NiO nanocomposites through the thermogravimetric analysis (TGA) measurement in the nitrogen gas environment. TGA was performed by an integrated thermal analyzer with a ramp rate of 20 °C min^{-1} under N_2 protection. Furthermore, X-ray diffraction (XRD) was used for analyzing the crystalline structure of the as-obtained sample. X-ray photoelectron spectroscopy (XPS) spectra were carried out to analyze the surface compositions and chemical valence information for the as-prepared sample. All binding energies were referred to as the C 1s peak of the surface adventitious carbon at 284.8 eV.

Electrochemical measurements

All electrochemical measurements of urea oxidation were performed on a CHI (760E, Texas, USA) electrochemical analyzer. The conventional three-electrode testing configuration was used in all electrochemical measurements. A glassy carbon electrode (Ø 3 mm) was used as the working electrode (WE) and would receive catalyst modification, Pt electrode and Ag/AgCl (within saturated KCl solution) were selected as counter and reference electrode (CE and RE), respectively. Considering different concentrations of urea used for oxidation, such as 0.1 M, 0.33 M and 0.5 M, 0.33 M urea was selected for oxidation measurements in this study to match the concentration in mammal urine.[42, 43] Cyclic voltammetry (CV) and linear sweep voltammetry (LSV) or polarization measurements were both carried out in a 1.0 M alkali solution within/without 0.33 M urea. Electrochemical impedance spectroscopy (EIS) spectrum was also investigated in 0.1 M potassium ferricyanide solution (frequency range: 100 kHz-0.1 Hz, AC perturbation: 5 mV, applied potential: open-circuit potential). Electrochemical double-layer capacitance (C_{dl}) tests

were performed through a series of CV tests using a series of scan rates (2-10 mV s^{-1}) in 1.0 KOH with a similar potential range (0.06-0.16 V *vs.* Ag/AgCl). Chronoamperometry (CA) measurements were carried out at a constant potential of oxidation peak potential *vs.* Ag/AgCl for 1800 s in 1.0 alkali media with 0.33 M urea. Here, the loading mass of the catalyst on the working electrode was calculated as 0.075 mg cm^{-2}, and all potentials mentioned in this study were converted versus a reversible hydrogen electrode (RHE): ($E_{RHE} = E_{Ag/AgCl} + 0.21\ V + 0.059 \times pH$, 25℃) unless otherwise specified, and *iR* compensation was performed for all linear LSV results.

DFT calculation methods

To study the source of the highly electrocatalytic performance of C@NiO nanocomposites, calculations were carried out using spin-polarized density functional theory (DFT), equipped with the CASTEP package with the Perdew-Burke-Ernzerh (PBE) of generalized gradient approximation (GGA) exchange-correlation functional.[44] The adsorption of urea and CO_2 on the C@NiO was studied compared with that on C@NiOOH, and the heterojunctions were chosen as our theoretical models. The core electrons were treated with Ultrasoft Pseudopotentials.[45] The cutoff energy for the plane wave expansion was 340 eV, and the Monkhorst-Pack k-point sampling was generated with a 2×2×1 grid. The convergence criterion for the structural optimizations was a maximum force of 0.05 eV/Å and a maximum displacement of 0.002 Å. A vacuum layer of 15 Å thickness was used along the z-direction to totally eliminate the interactions between different surfaces. The adsorption energy of urea or CO_2 over C@NiO and C@NiOOH was calculated according to the Equation.1:

$$E_{ads} = E_{total} - (E_{slab} + E_{adsorbate}) \quad (1)$$

Where E_{ads} is the adsorption energy, E_{total} is the total energy for the adsorption state, E_{slab} is the energy of the optimized surface of C@NiO or C@NiOOH and $E_{adsorbate}$ is the energy of mono urea or CO_2 molecule.

Results and discussion

Physical characterizations of the porous C@NiO nanocomposites

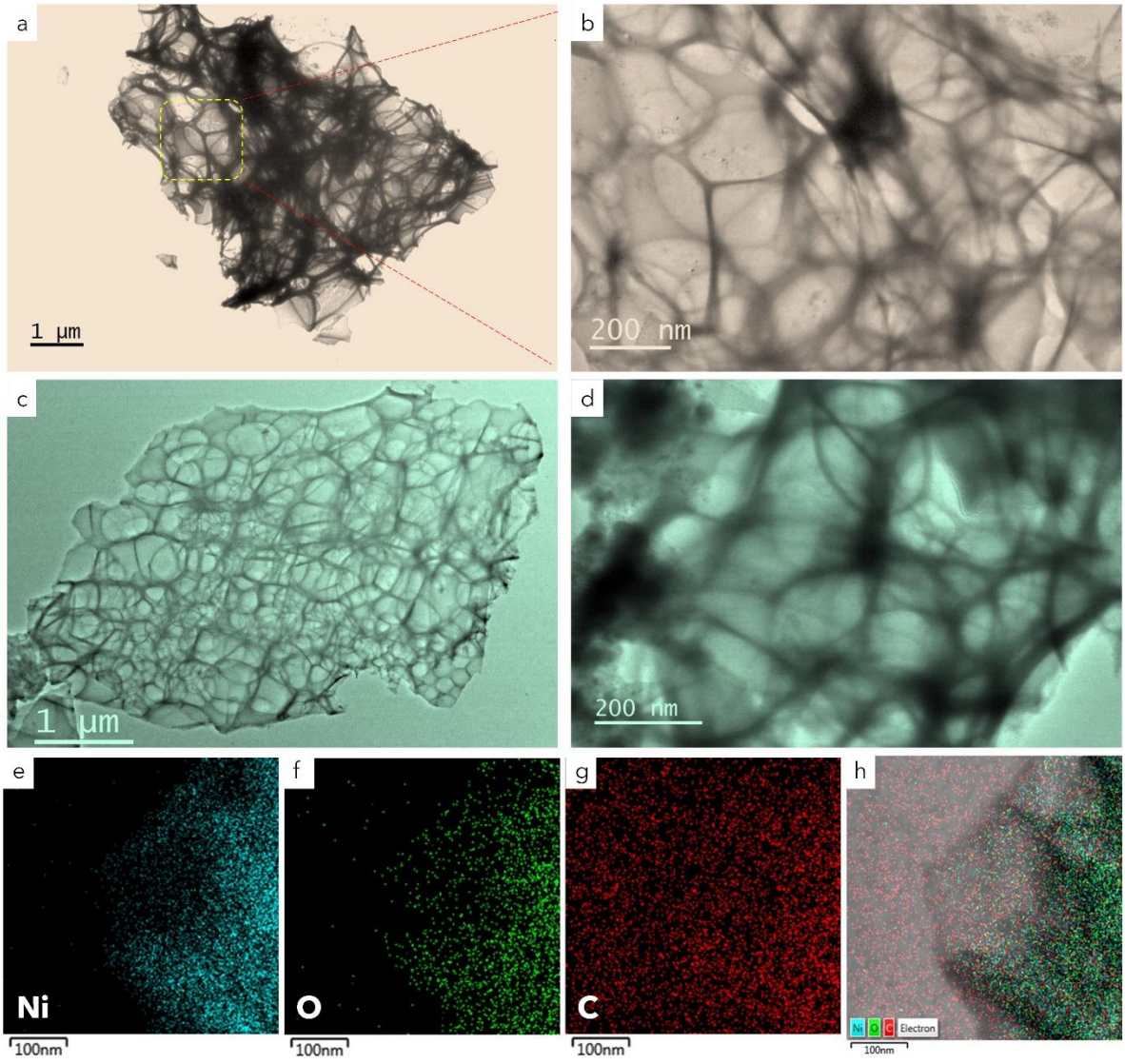

Figure 2. (a-b) TEM images of the porous carbon. (c-d) TEM images and (e-h) STEM-EDX images of the C@NiO nanocomposites.

There is a hierarchical structure of the porous carbon with transparent layers between carbon frameworks (**Figs. 2a-b**), indicating that it can provide a large surface area for active sites.[46] As depicts in **Fig. 2c**, NiO nanoparticles are anchored on the porous carbon frameworks. The color of carbon layers tends to dark (**Fig. 2d**) which differs from **Fig. 2b**. This phenomenon may be due to the introduction of NiO nanoparticles. STEM-EDX mapping was further applied to verify the composition of the as-prepared sample. The element distribution of Ni, O and C without other impurities on the transparent layers is observed well with higher magnification (~100 nm) in **Figs. 2e-h**. That porous structure is derived from the biomacromolecule fibers of ESM[38], with NiO nanoparticles dispersed well on the porous carbon, as presents in **Fig. 2g**.

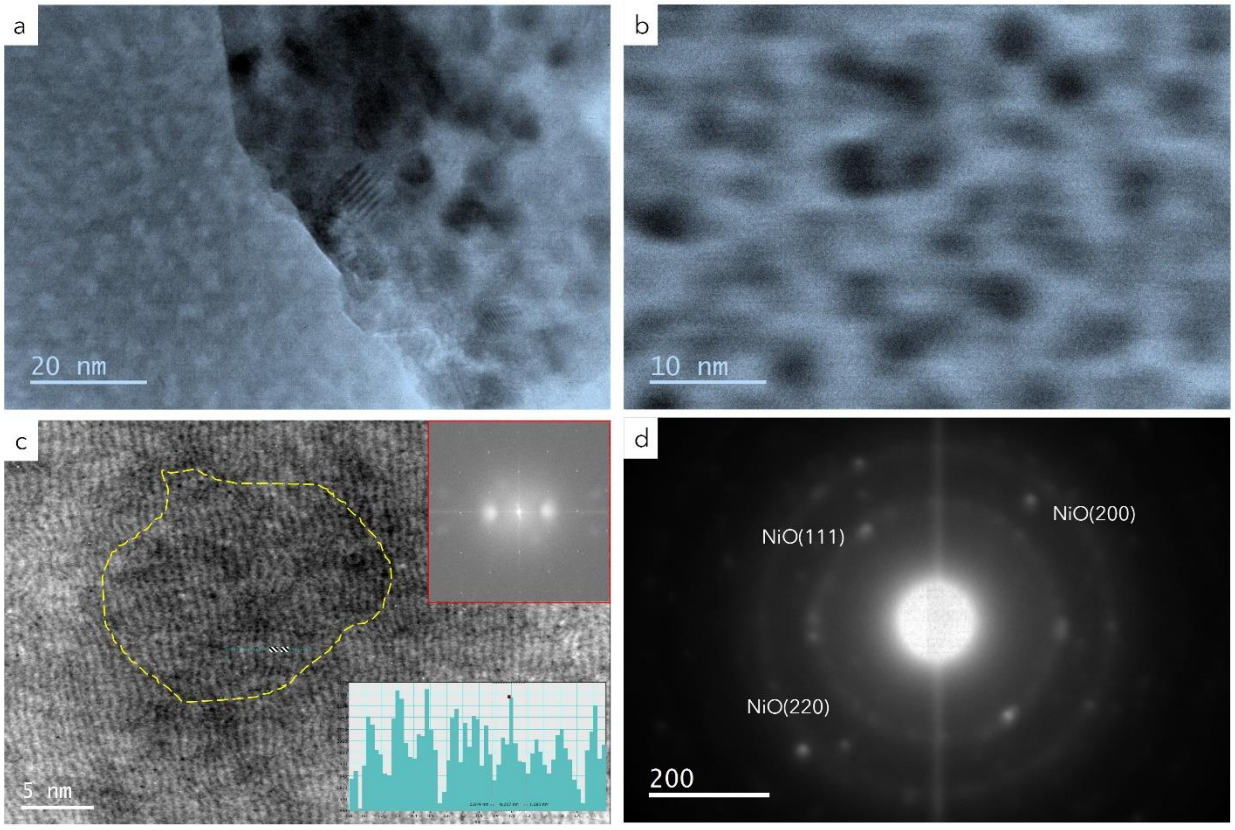

Figure 3. (a-b) TEM images with magnifications (20 nm and 10 nm), (c) HRTEM image and (d) SAED pattern of C@NiO nanocomposites.

Several black dots with an average size of 6.5 nm are displayed in **Figs. 3a-b**, confirming the existence of NiO nanoparticles. **Fig. 3c** exhibits the average lattice spacing of 0.207 nm in the dark area, which corresponds to the (111) fact of NiO (JCPDS No.47-1049). **Fig. S1** also presents several similar areas with the same lattice spacing from **Fig. 3c**. Meanwhile, NiO grains encapsulated on the porous carbon also can be confirmed by its lattice fringes using fast Fourier transform (FFT) of HRTEM image due to NiO having specified unit cell parameters of 0.418 nm with face-centered cubic (fcc) structures (inset of **Fig. 3c**). As a comparison, pure NiO particles were synthesized using the same method and their morphology appeared aggregation with different sizes (**Fig. S2**) due to no supports in hydrothermal treatment for good dispersion.[47] The SAED result of C@NiO nanocomposites in **Fig. 3d** reveals the polycrystalline property with the feature of uniform central and diffraction spots. The diffraction rings have corresponded to the diffraction of the graphite-like carbon and the appeared spots are indexed to (111), (200), and (220) diffraction of pure NiO. All the above results demonstrated the porous C@NiO nanocomposite was successfully prepared with hierarchical structure and uniform dispersion.

TGA result of the precursor $Ni(OH)_2$/ESM is presented in **Fig. S3**. The precursor $Ni(OH)_2$/ESM endured a four-step weight loss owing to continuous dehydration and decomposition. The first stage (20-100 °C) is related to the evaporation of the adsorbed and intercalated water molecules associated with the surface of $Ni(OH)_2$/ESM. It is possible to estimate the water content (10 *wt.*%) of the precursor. ESM started pyrolyzing at ~200 °C and was completely pyrolyzed at 550 °C with a weight loss of 48 *wt.*%. Similarly, Zhai et al. found that decomposition of $Ni(OH)_2$ into NiO occurs between 300 and 400 °C.[48] For this step, the TG curve exhibits a sharp weight loss with 19 *wt.*%, which is in line with the theoretical weight loss value (19.4%) due to the decomposition of $Ni(OH)_2$.[49] Organic components are completely removed in

this stage, including gas like CO_2, resulting in the uniformed NiO nanoparticles anchoring on the porous carbon. This result keeps consistent with previous TEM and SEM observations well.

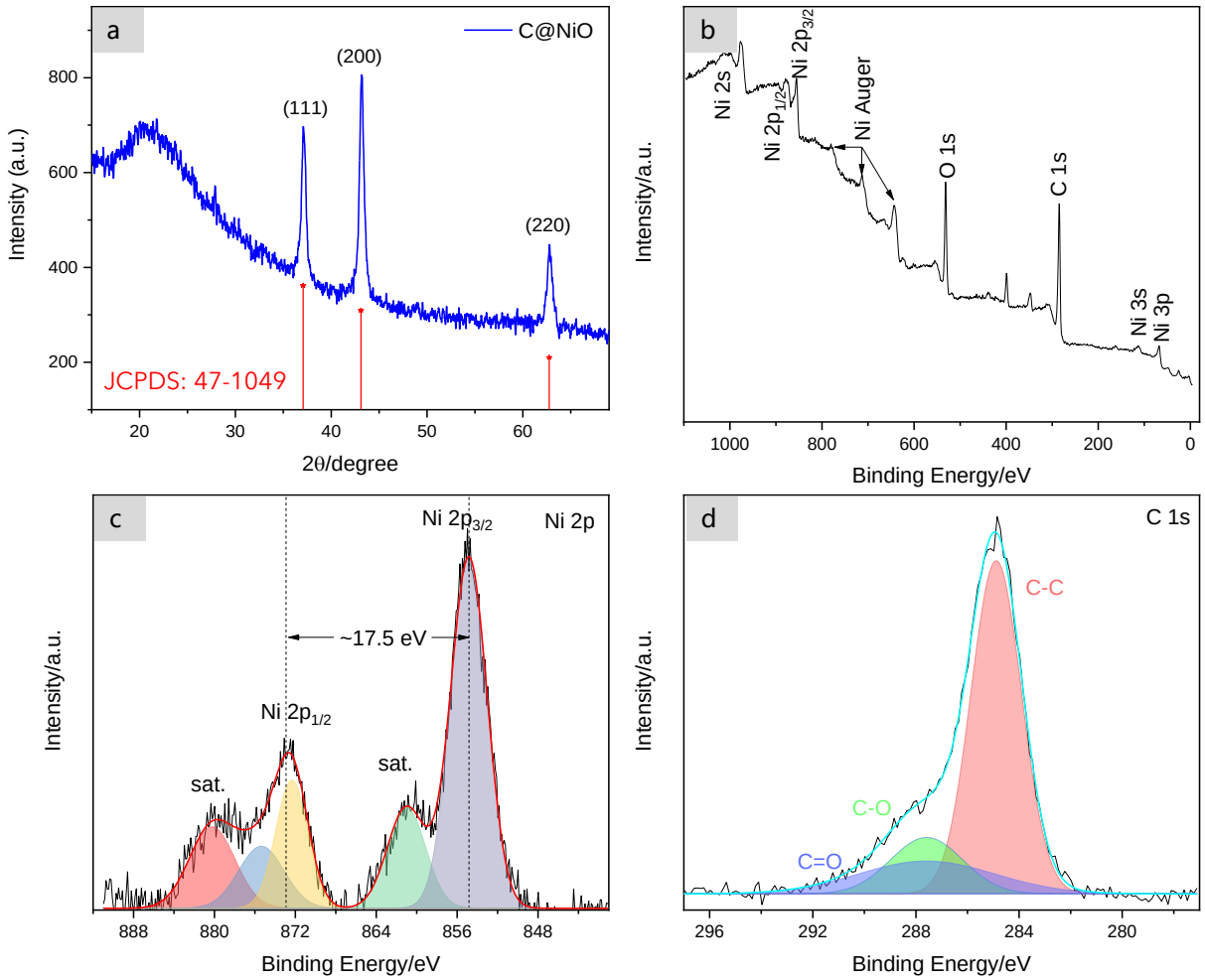

Figure 4. (a) XRD pattern, (b) XPS survey spectrum, and the high-resolution XPS spectra of (c) Ni 2p and (d) C 1s regions, of C@NiO nanocomposites.

In **Fig. 4a**, the peaks appeared in 37.2°, 43.2°, 62.8° (2θ) are indexed to the crystal planes of NiO (JCPDS Card #47-1049) well. The peaks at 24.8° also confirmed the existence of carbon (JCPDS Card #41-1487). This XRD analysis identified the presence of NiO and C in the as-prepared sample, which also keeps consistent with the HRTEM pattern. The XPS survey spectrum of C@NiO nanocomposites further confirms the existence of nickel, oxygen, and carbon species

in **Fig. 4b**. There are two apparent peaks located at 873.3 eV and 855.8 eV due to Ni $2p_{1/2}$ and Ni $2p_{3/2}$, as depicted in **Fig. 4c**. As a result, the binding energy peaks at 880 eV and 861 eV are assigned to the satellite peaks of Ni $2p_{1/2}$ and Ni $2p_{3/2}$, respectively. The spin-energy separation of two main peaks (from 873.3 eV to 855.8 eV) is ~17.5 eV, which is the typical characteristic of the $Ni(OH)_2$ phase[48], Nevertheless, all the Ni 2p peaks of the as-prepared sample shift to higher binding energies compared to $Ni(OH)_2$, implying a higher oxidation state of Ni(II) ions in C@NiO nanocomposites.[13] The C 1s can be further fitted to three peaks located at 286.4, 285.8, and 284.2 eV, corresponding to carbonyl bond, carbon-oxygen bond, and carbon-carbon bond in **Fig. 4d**. The above results further confirmed that the successful growth of NiO nanoparticles anchored on the porous carbon to prepare C@NiO nanocomposites.

UOR performance of the porous C@NiO nanocomposites

To assess the electrocatalytic performance of C@NiO nanocomposites for urea oxidation, electrochemical measurements were applied through a typical three-electrode setting. Urea electrolysis reaction in alkaline environmental can be expressed as following (Equations.2-4):

Anode: $CO(NH_2)_2 + 6OH^- \rightarrow N_2 + 5H_2O + CO_2 + 6e^-$ (2)

Cathode: $2H_2O + 2e^- \rightarrow H_2 + 2OH^-$ (3)

Overall: $CO(NH_2)_2 + H_2O \rightarrow N_2 + 3H_2 + CO_2$ (4)

The electrochemical behaviours of the C@NiO electrode were evaluated by CV measurements in the alkaline medium in the absence/presence of 0.33 M urea, and the pure NiO sample and the porous carbon electrode were also tested for comparison, as shown in **Fig. S4.** As for C@NiO electrode, there is an obvious oxidation peak at ~1.32 V, which can be attributed to the formation of NiOOH species.[25] However, C@NiO electrode presents an improved current density for urea

oxidation after the addition of urea. Coincidentally, the onset potential of UOR is very close to the potential position where NiOOH species are generated, implying that the fresh NiOOH species acted as active sites for urea oxidation, which is in consistent with the reported Ni-based electrocatalysts.[13, 41, 47, 50] Furthermore, the integrated area of the CV of C@NiO electrode is larger than the porous carbon electrode, indicating that NiO nanoparticles anchoring the porous carbon exposed more active species for urea oxidation and enhanced the electrocatalytic performance of UOR. **Fig. 5a** reveals the linear sweep voltammetry curves of C@NiO electrode compared with the porous carbon and commercial 20% Pt/C in the alkali media containing 0.33 M urea. The current density of C@NiO electrode increases with the potential move towards the positive side, while the other two samples only show minor changes. The UOR catalytic performance of C@NiO is estimated by Tafel curves in **Fig. 5b**. A more intuitional comparison of potential (the current density of 10 mA cm^{-2}) and Tafel information among C@NiO electrode, the porous carbon and commercial 20% Pt/C could be found in the histogram (**Fig. 5c**), in which C@NiO electrode presents the lowest potential to attain 10 mA cm^{-2}. The Tafel slope of C@NiO (87.2 mV dec^{-1}) is also lower than those of the porous carbon and commercial Pt/C, implying faster UOR kinetics for C@NiO electrode. As presented in **Table S1**, UOR performance of several electrocatalysts was listed. The C@NiO electrode presents a smaller potential and lower mass loading than that of the porous carbon and commercial Pt/C, suggesting its favorable reaction kinetics for UOR.

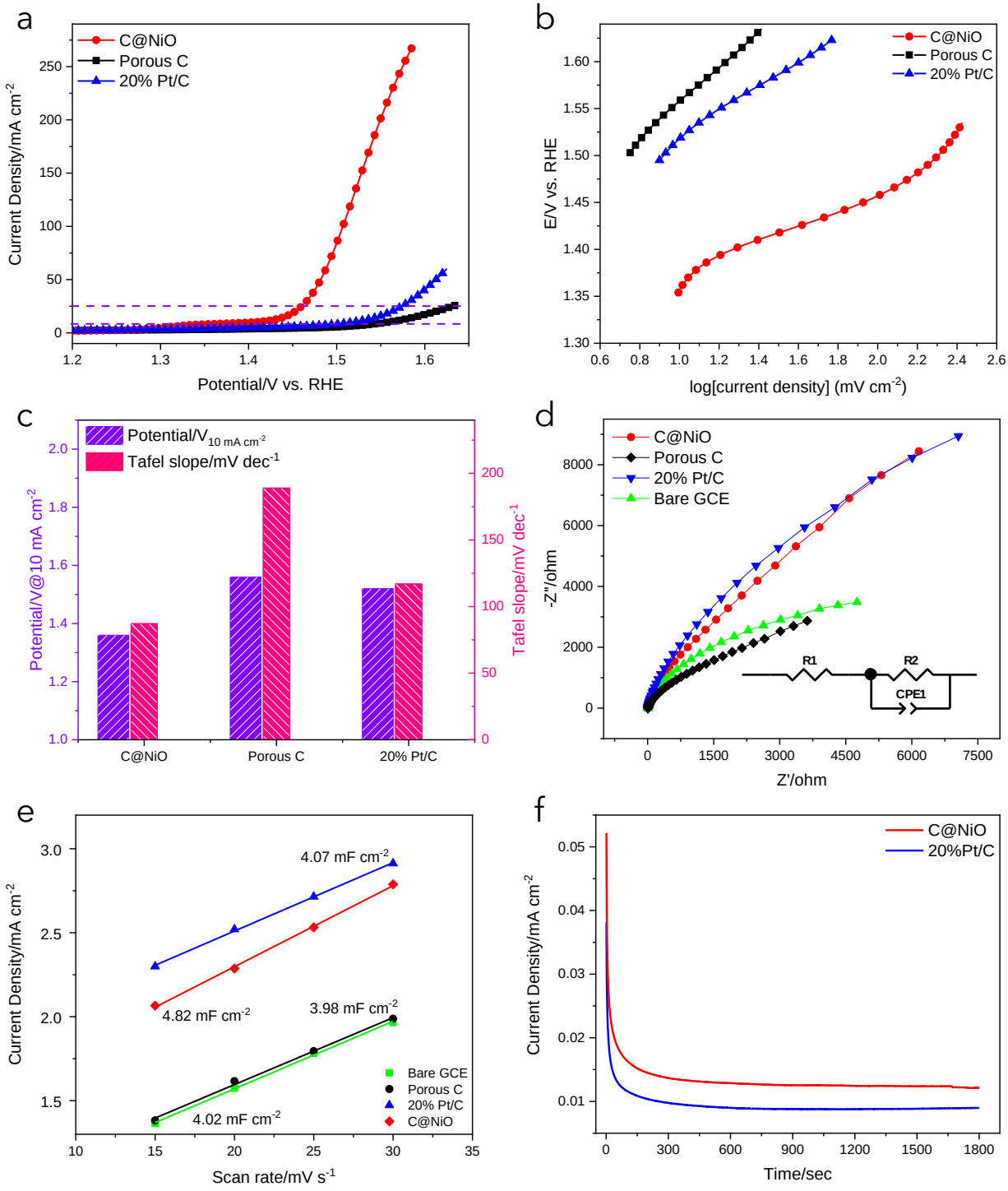

Figure 5. Electrochemical performance for UOR. (a) LSV curves of the porous carbon, 20% Pt/C and C@NiO electrodes in 1.0 M KOH containing 0.33 M urea, (b) Tafel plots of the above samples, (c) The histogram of a comparison of the potentials and Tafel slopes between the porous carbon, 20% Pt/C and C@NiO electrodes, (d) Nyquist plots of the porous carbon, 20% Pt/C and C@NiO electrodes in 1.0 M KOH with an open circuit voltage, (e) Linear plots of double-layer capacitance to assess the electrochemically active surface area, (f) Chronoamperometry curves of C@NiO and 20% Pt/C in the 1.0 M KOH containing 0.33 M urea at an applied potential of 1.3 V (*vs.* RHE).

Mechanism investigation via electrochemical measurements

EIS measurement was also tested to obtain more information about the catalytic performance of C@NiO nanocomposites. The porous carbon, 20% Pt/C and the bare GCE were all received the same test as comparison. The results presented in **Fig. 5d** indicate that C@NiO electrode presents a much smaller Nyquist semicircle than that of the porous carbon, 20% Pt/C and the bare GCE under an open-circuit potential, revealing that it has a much faster charge transfer than other samples, which is well matched with the previous polarization curves. Electrochemical active surface area (ECSA) measurements were further performed to study the electrochemical double-layer capacitance (C_{dl}) among C@NiO, the porous carbon, 20% Pt/C and the bare GCE. As demonstrated in **Fig. 5e**, C@NiO electrode was calculated to be 4.82 mF cm^{-2}, well above the values of the porous carbon (3.98 mF cm^{-2}), 20% Pt/C (4.07 mF cm^{-2}) and the bare GCE (4.02 mF cm^{-2}). Calculation details can be found in **Fig. S5**. This means C@NiO electrode has larger active surface area with more active sites that promote UOR efficiently. In addition, the presence of urea increases the current density of the anode as the potential is also applied. As presented in **Fig. S6,** the current density of C@NiO electrode presents the increasing stepwise potential in 1.0 M alkali solution with/without 0.33 M urea. When the positive potential (0.1-0.4 V *vs.* Ag/AgCl) was applied, there are no redox cycles corresponding to the conversion of Ni^{2+} species to Ni^{3+} species before urea addition. When the potential (0.5-0.8 V *vs.* Ag/AgCl) larger than the onset potential was applied, a higher current density can be obtained owing to the OER effect. It can be inferred that the porous C@NiO nanocomposites induce a high electron transfer and mass transport due to their excellent electrical conductivity.

Moreover, the stable multistep chronopotentiometry (CP) curves also suggest the better conductivity and mass transport of C@NiO electrode for UOR performance. The stability of

C@NiO electrode during urea oxidation was further examined, as shown in **Fig. 5f**. It can be observed that the current density of C@NiO electrode only shows negligible degradation compared with the commercial 20% Pt/C after 1800 s testing under an applied potential of 1.3 V *vs.* RHE. This indicates that C@NiO electrode has good catalytic stability in alkali with urea. To further confirm the structural stability after long-term durability, the stripped sample from the working electrode was observed again by the TEM technique. It keeps the original layer structure with uniform NiO nanoparticles, as demonstrated in **Fig. S7**. Consequently, it can be concluded that C@NiO electrode shows excellent UOR performance owing to i) NiO nanoparticles directly anchored on the porous carbon could enlarge the electrochemically active surface area; ii) the transparent carbon layer could enhance its electrical conductivity, providing faster electron transfer and mass transport between nanoparticles and the carbon matrix, improving UOR electrocatalytic performance, reducing NiO nanoparticles contact with electrolyte directly, thereby enhancing the stability.

Mechanism investigation via theoretical calculations

To gain insight into the synergistic effect in C@NiO nanocomposites towards urea oxidation, spin-polarized DFT calculations were utilized to provide more details in this work. Generally, $CO(NH_2)_2$ is primarily adsorbed on the surface of electrocatalysts during urea electrooxidation. It indicates that the adsorption energy of urea plays an important function in determining the electrocatalytic urea oxidation[51]. It is noteworthy that our DFT calculations do not take all the experimental details into account, and the graphene was present as an alternative structure to simulate the porous carbon, qualitatively revealing the influence of the porous structure on the electronic structure of NiO nanoparticles. The graphene/NiOOH and graphene/NiO heterojunctions were chosen as the theoretical models in this work (**Figs. 6a-b**). According to the

DFT calculations, the urea preferred to adsorb on the surface of C@NiOOH heterojunction and the adsorption energy is -1.53 eV, while the adsorption energy is only -0.97 eV on the C@NiO heterojunction (**Fig. S8a**). Moreover, the electron density difference as shown in **Figs. 6c-d**, and the slice of electron density difference in **Figs. 6e-f** showed that a little bit more electrons from Ni transferring to the O atom of urea on the C@NiOOH heterojunction than that on C@NiO heterojunction, which means that the alkaline environment plays an important role in the UOR. And it can be deemed that the Ni(III) species presented its favorable active sites.

Besides, CO_2 adsorption on the surface or interface of catalysts is significant to the remarkable UOR performance[52]. Moreover, the rate-determining step in UOR is the adsorbed CO_2 desorption from active sites[53]. Thus, the adsorption energy of CO_2 on C@NiO electrode and C@NiOOH was comparatively studied with DFT calculations. As illustrated in **Fig. S8b**, it can be determined that the adsorption energy of CO_2 on the C@NiO is -0.57 eV, while it becomes almost zero on the C@NiOOH surface, which means a much weaker CO_2 adsorption over C@NiOOH. Furthermore, the calculated d band center of Ni in C@NiO is -1.97 eV, while it goes far from the Fermi level and decreases to -2.20 eV for the Ni in C@NiOOH (**Fig. S8c**). The lower d band center leads to the weaker adsorption for CO_2. From this viewpoint, it enables to effectively retard the "CO_2 poisoning" of electrocatalyst, ensuring its superior UOR performance.

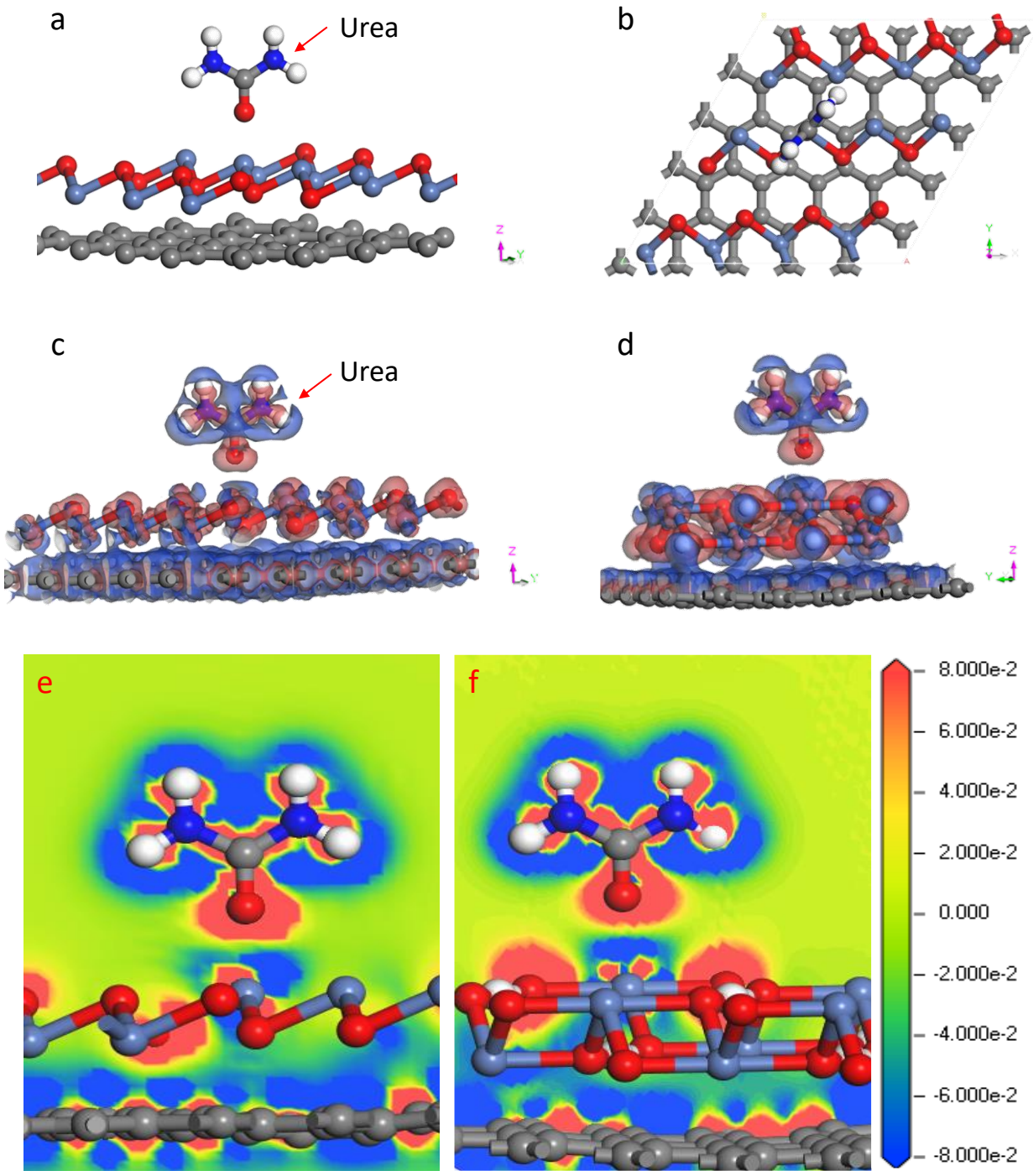

Figure 6. The structural model of the porous C@NiO and urea under different views (a-b). The electron density difference of urea adsorbed on (c) C@NiO and (d) C@NiOOH, the red hooded face means enrichment of electrons while the blue one means the deficiency of electrons. Slice images of the adsorption of urea molecule on the surface of (e) C@NiO and (f) C@NiOOH heterojunctions and the corresponding slice of electron density difference. The contour around the atoms represents the electron accumulation (red) or electron deletion (blue).

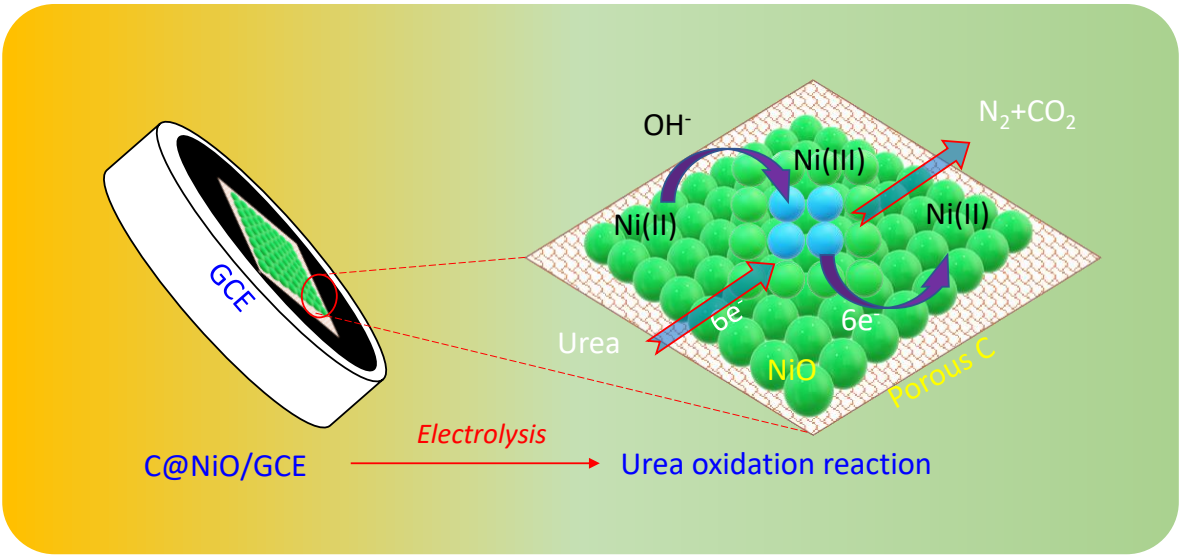

Figure 7. The mechanism of UOR on C@NiO electrode.

UOR performance enhancement mechanism discussion

The improvement of UOR performance is mainly benefited from the synergistic effect between NiO and the porous carbon, as illustrated in **Fig. 7**. It can be ascribed to several reasons, as follows: *i)* NiO nanoparticles directly encapsulated onto the porous carbon enlarged the electrochemically active surface area with more active sites. For example, 3D interwoven-like structure could afford more active sites and enable gas release for reactions in the viewpoint of material preparation. *ii)* The transparent carbon layer could enhance its electrical conductivity, providing faster electron transfer and mass transport between nanoparticles and the carbon matrix, improving UOR electrocatalytic performance, reducing NiO nanoparticles contact with electrolyte directly, therefore enhancing the stability. *iii)* The synergistic effect in C@NiO nanocomposites could regulate the electron density to optimize active sites and promote electrocatalytic UOR performance efficiently in terms of theoretical calculations.

Conclusion

In summary, we have reported the nickel oxide nanoparticles supported on the carbonized eggshell membrane with interwoven networks as low-cost electrocatalysts (C@NiO) toward urea oxidation. The resultant C@NiO electrode exhibited much better electrocatalytic urea oxidation performance than that of the commercial 20% Pt/C under the same test conditions. It can achieve a current density of 10 mA cm^{-2} at 1.36 V (*vs.* RHE) and 25 mA cm^{-2} at 1.46 V (*vs.* RHE) and a low Tafel slope of 87.2 mV dec^{-1}. Such an excellent urea oxidation performance could be attributed to the synergetic effect in the porous carbon and NiO nanoparticles which provides excellent electrocatalytic activity and stability in the C@NiO nanocomposites. Moreover, benefiting from theoretical calculations, Ni(III) species and the porous carbon further enabled the electrocatalyst to effectively inhibit the "CO_2 poisoning" of electrocatalysts, guaranteeing its superior UOR performance. This study may promote the low-cost UOR electrocatalyst design with porous structure and uniform composition and develop biomass-derived applications in urea conversion based on the concept of "trash to treasure".

Supporting information

HRTEM image of C@NiO nanocomposites; SEM images of NiO particles and the porous carbon; TGA curve of C@NiO nanocomposites; comparison of CV results for NiO, the porous carbon and C@NiO nanocomposites in the absence and presence of urea in the alkaline solution; CV curves of the GCE, the porous carbon, Pt/C and C@NiO nanocomposites in a narrow range; the current response at the different potential on the C@NiO electrode; TEM images of C@NiO nanocomposites after urea oxidation; The adsorption energy of urea/CO_2 on the porous C@NiO

and C@NiOOH; The d density of states of Ni in NiO and NiOOH; and comparison of the UOR performance and mass loadings between recently reported electrocatalysts.

Author information

Corresponding Authors

Zhengrong Gu – Department of Agricultural and Biosystems Engineering, South Dakota State University, Brookings, SD, 57007, USA; orcid.org/0000-0003-1860-2651; Email: zhengrong.gu@sdstate.edu

Xueqiang Qi - College of Chemistry and Chemical Engineering, Chongqing University of Technology, Chongqing, 400054, China; Email: xqqi@cqut.edu.cn

Xiaoteng Liu - Department of Mechanical & Construction Engineering, Faculty of Engineering and Environment, Northumbria University, Newcastle upon Tyne, NE1 8ST, UK; orcid.org/ 0000-0001-7574-1709; Email: Terence.liu@northumbria.ac.uk

Authors:

Shun Lu - Department of Agricultural and Biosystems Engineering, South Dakota State University, Brookings, SD, 57007, USA

Matthew Hummel - Department of Agricultural and Biosystems Engineering, South Dakota State University, Brookings, SD, 57007, USA

Yucheng Wang - Department of Mechanical & Construction Engineering, Faculty of Engineering and Environment, Northumbria University, Newcastle upon Tyne, NE1 8ST, UK

Keliang Wang - Department of Electrical Engineering and Computer Engineering & Department of Chemical Engineering and Materials Science, Michigan State University, East Lansing, MI, 48824, USA

Rajesh Pathak - Department of Electrical Engineering and Computer Science, South Dakota State University, Brookings, SD, 57007, USA

Yue Zhou - Department of Electrical Engineering and Computer Science, South Dakota State University, Brookings, SD, 57007, USA

Hongxing Jia - Department of Agricultural and Biosystems Engineering, South Dakota State University, Brookings, SD, 57007, USA

Xianhui Zhao - Manufacturing Science Division, Oak Ridge National Laboratory, 1 Bethel Valley Road, Oak Ridge, Tennessee, 37831, USA

Ben Bin Xu - Department of Mechanical & Construction Engineering, Faculty of Engineering and Environment, Northumbria University, Newcastle upon Tyne, NE1 8ST, UK

Notes

The authors declare no competing financial interests.

Acknowledgements

This work is supported by NASA EPSCoR (No. NNX16AQ98A), NSF/EPSCoR (No. OIA-1849206), the UK Engineering Physics and Science Research Council (Grant No. EP/S032886/1), the Foundation and Frontier Research Project of Chongqing of China (cstc2018jcyjAX0513) and the Science and Technology Research Program of Chongqing Municipal Education Commission (KJQN201801125). In addition, S. Lu thanks for Miss. Yuehui Wang's care during Shun's Ph.D. period. This manuscript has been authored in part by UT-Battelle, LLC, under contract DE-AC05-00OR22725 with the US Department of Energy (DOE). The US government retains and the publisher, by accepting the article for publication, acknowledges that the US government retains a nonexclusive, paid-up, irrevocable, worldwide license to publish or reproduce the published form of this manuscript, or allow others to do so, for US government purposes. DOE will provide public access to these results of federally sponsored research in accordance with the DOE Public Access Plan (http://energy.gov/downloads/doe-public-access-plan).

References

1. Zhang, J.-Y.; He, T.; Wang, M.; Qi, R.; Yan, Y.; Dong, Z.; Liu, H.; Wang, H.; Xia, B. Y., Energy-saving hydrogen production coupling urea oxidation over a bifunctional nickel-molybdenum nanotube array. *Nano Energy* **2019,** *60*, 894-902, DOI 10.1016/j.nanoen.2019.04.035.

2. Rollinson, A. N.; Jones, J.; Dupont, V.; Twigg, M. V., Urea as a hydrogen carrier: a perspective on its potential for safe, sustainable and long-term energy supply. *Energy Environ. Sci.* **2011,** *4* (4), 1216-1224, DOI 10.1039/C0EE00705F.

3. Chen, S.; Duan, J.; Vasileff, A.; Qiao, S. Z., Size Fractionation of Two-Dimensional Sub-Nanometer Thin Manganese Dioxide Crystals towards Superior Urea Electrocatalytic Conversion. *Angew. Chem., Int. Ed.* **2016,** *55* (11), 3804-3808, DOI 10.1002/anie.201600387.

4. Sha, L.; Ye, K.; Wang, G.; Shao, J.; Zhu, K.; Cheng, K.; Yan, J.; Wang, G.; Cao, D., Hierarchical $NiCo_2O_4$ nanowire array supported on Ni foam for efficient urea electrooxidation in alkaline medium. *J. Power Sources* **2019,** *412*, 265-271, DOI 10.1016/j.jpowsour.2018.11.059.

5. Yue, Z. H.; Yao, S. Y.; Li, Y. Z.; Zhu, W. X.; Zhang, W. T.; Wang, R.; Wang, J.; Huang, L. J.; Zhao, D. Y.; Wang, J. L., Surface engineering of hierarchical $Ni(OH)_2$ nanosheet@nanowire configuration toward superior urea electrolysis. *Electrochim. Acta* **2018,** *268*, 211-217, DOI 10.1016/j.electacta.2018.02.059.

6. Urbańczyk, E.; Maciej, A.; Stolarczyk, A.; Basiaga, M.; Simka, W., The electrocatalytic oxidation of urea on nickel-graphene and nickel-graphene oxide composite electrodes. *Electrochim. Acta* **2019,** *305*, 256-263, DOI 10.1016/j.electacta.2019.03.045.

7. Radenahmad, N.; Afif, A.; Petra, P. I.; Rahman, S. M.; Eriksson, S.-G.; Azad, A. K., Proton-conducting electrolytes for direct methanol and direct urea fuel cells–A state-of-the-art review. *Renew. Sust. Energ. Rev.* **2016,** *57*, 1347-1358, DOI 10.1016/j.rser.2015.12.103.

8. Nguyen, N. S.; Das, G.; Yoon, H. H., Nickel/cobalt oxide-decorated 3D graphene nanocomposite electrode for enhanced electrochemical detection of urea. *Biosens. Bioelectron.* **2016,** *77*, 372-377, DOI 10.1016/j.bios.2015.09.046.

9. Yu, Z.-Y.; Lang, C.-C.; Gao, M.-R.; Chen, Y.; Fu, Q.-Q.; Duan, Y.; Yu, S.-H., Ni–Mo–O nanorod-derived composite catalysts for efficient alkaline water-to-hydrogen conversion via urea electrolysis. *Energy Environ. Sci.* **2018,** *11* (7), 1890-1897, DOI 10.1039/C8EE00521D.

10. Yan, W.; Wang, D.; Botte, G. G., Electrochemical decomposition of urea with Ni-based catalysts. *Appl. Catal., B* **2012,** *127*, 221-226, DOI 10.1016/j.apcatb.2012.08.022.

11. Jia, H.; Yao, Y.; Zhao, J.; Gao, Y.; Luo, Z.; Du, P., A novel two-dimensional nickel phthalocyanine-based metal–organic framework for highly efficient water oxidation catalysis. *J. Mater. Chem. A* **2018,** *6* (3), 1188-1195, DOI 10.1039/C7TA07978H.

12. Zhan, S.; Zhou, Z.; Liu, M.; Jiao, Y.; Wang, H., 3D NiO nanowalls grown on Ni foam for highly efficient electro-oxidation of urea. *Catal. Today* **2019,** *327*, 398-404, DOI 10.1016/j.cattod.2018.02.049.

13. Zhu, D.; Guo, C.; Liu, J.; Wang, L.; Du, Y.; Qiao, S.-Z., Two-dimensional metal–organic frameworks with high oxidation states for efficient electrocatalytic urea oxidation. *Chem. Commun. (Cambridge, U.K.)* **2017,** *53* (79), 10906-10909, DOI 10.1039/C7CC06378D.

14. Ma, G.; Xue, Q.; Zhu, J.; Zhang, X.; Wang, X.; Yao, H.; Zhou, G.; Chen, Y., Ultrafine Rh nanocrystals decorated ultrathin NiO nanosheets for urea electro-oxidation. *Appl. Catal., B* **2020,** *265*, 118567, DOI 10.1016/j.apcatb.2019.118567.

15. Wang, Z.; Liu, W.; Hu, Y.; Guan, M.; Xu, L.; Li, H.; Bao, J.; Li, H., Cr-doped CoFe layered double hydroxides: Highly efficient and robust bifunctional electrocatalyst for the oxidation of water and urea. *Appl. Catal., B* **2020,** *272*, 118959, DOI 10.1016/j.apcatb.2020.118959.

16. Sayed, E. T.; Eisa, T.; Mohamed, H. O.; Abdelkareem, M. A.; Allagui, A.; Alawadhi, H.; Chae, K.-J., Direct urea fuel cells: Challenges and opportunities. *J. Power Sources* **2019,** *417*, 159-175, DOI 10.1016/j.jpowsour.2018.12.024.

17. Simka, W.; Piotrowski, J.; Nawrat, G., Influence of anode material on electrochemical decomposition of urea. *Electrochim. Acta* **2007,** *52* (18), 5696-5703, DOI 10.1016/j.electacta.2006.12.017.

18. Baker, D. R.; Lundgren, C. A., Expansion of the urea electrocatalytic oxidation window by adsorbed nickel ions. *J. Appl. Electrochem.* **2019,** *49* (9), 883-893, DOI 10.1007/s10800-019-01328-9.

19. Yue, Z.; Zhu, W.; Li, Y.; Wei, Z.; Hu, N.; Suo, Y.; Wang, J., Surface engineering of a nickel oxide–nickel hybrid nanoarray as a versatile catalyst for both superior water and urea oxidation. *Inorg. Chem.* **2018,** *57* (8), 4693-4698, DOI 10.1021/acs.inorgchem.8b00411.

20. Yang, W.; Yang, X.; Hou, C.; Li, B.; Gao, H.; Lin, J.; Luo, X., Rapid room-temperature fabrication of ultrathin $Ni(OH)_2$ nanoflakes with abundant edge sites for efficient urea oxidation. *Appl. Catal., B* **2019,** *259*, 118020, DOI 10.1016/j.apcatb.2019.118020.

21. Yang, W.; Yang, X.; Li, B.; Lin, J.; Gao, H.; Hou, C.; Luo, X., Ultrathin nickel hydroxide nanosheets with a porous structure for efficient electrocatalytic urea oxidation. *J. Mater. Chem. A* **2019,** *7* (46), 26364-26370, DOI 10.1039/C9TA06887B.

22. Yuan, M.; Wang, R.; Sun, Z.; Lin, L.; Yang, H.; Li, H.; Nan, C.; Sun, G.; Ma, S., Morphology-Controlled Synthesis of Ni-MOFs with Highly Enhanced Electrocatalytic Performance for Urea Oxidation. *Inorg. Chem.* **2019,** *58* (17), 11449-11457, DOI 10.1021/acs.inorgchem.9b01124.

23. Vedharathinam, V.; Botte, G. G., Understanding the electro-catalytic oxidation mechanism of urea on nickel electrodes in alkaline medium. *Electrochim. Acta* **2012,** *81*, 292-300, DOI 10.1016/j.electacta.2012.07.007.

24. Wang, D.; Yan, W.; Botte, G. G., Exfoliated nickel hydroxide nanosheets for urea electrolysis. *Electrochem. Commun.* **2011,** *13* (10), 1135-1138, DOI 10.1016/j.elecom.2011.07.016.

25. Boggs, B. K.; King, R. L.; Botte, G. G., Urea electrolysis: direct hydrogen production from urine. *Chem. Commun. (Cambridge, U.K.)* **2009,** (32), 4859-4861, DOI 10.1039/B905974A.

26. Yan, W.; Wang, D.; Botte, G. G., Nickel and cobalt bimetallic hydroxide catalysts for urea electro-oxidation. *Electrochim. Acta* **2012,** *61*, 25-30, DOI 10.1016/j.electacta.2011.11.044.

27. Yan, W.; Wang, D.; Diaz, L. A.; Botte, G. G., Nickel nanowires as effective catalysts for urea electro-oxidation. *Electrochim. Acta* **2014,** *134*, 266-271, DOI 10.1016/j.electacta.2014.03.134.

28. Ye, K.; Zhang, D.; Guo, F.; Cheng, K.; Wang, G.; Cao, D., Highly porous nickel@carbon sponge as a novel type of three-dimensional anode with low cost for high catalytic performance of urea electro-oxidation in alkaline medium. *J. Power Sources* **2015,** *283*, 408-415, DOI 10.1016/j.jpowsour.2015.02.149.

29. Shi, W.; Sun, X. J.; Ding, R.; Ying, D. F.; Huang, Y. F.; Huang, Y. X.; Tan, C. N.; Jia, Z. Y.; Liu, E. H., Trimetallic NiCoMo/graphene multifunctional electrocatalysts with moderate

structural/electronic effects for highly efficient alkaline urea oxidation reaction. *Chem. Commun. (Cambridge, U.K.)* **2020,** *56* (48), 6503-6506, DOI 10.1039/D0CC02132F.

30. Li, B.; Song, C.; Rong, J.; Zhao, J.; Wang, H.-E.; Yang, P.; Ye, K.; Cheng, K.; Zhu, K.; Yan, J., A new catalyst for urea oxidation: $NiCo_2S_4$ nanowires modified 3D carbon sponge. *J. Energy Chem.* **2020,** *50*, 195-205, DOI 10.1016/j.jechem.2019.12.018.

31. Cook, B., Introduction to fuel cells and hydrogen technology. *Eng. Sci. Educ. J* **2002,** *11* (6), 205-216, DOI 10.1049/esej:20020601.

32. Mekhilef, S.; Saidur, R.; Safari, A., Comparative study of different fuel cell technologies. *Renew. Sust. Energ. Rev.* **2012,** *16* (1), 981-989, DOI 10.1016/j.rser.2011.09.020.

33. Zhu, B.; Liang, Z.; Zou, R., Designing Advanced Catalysts for Energy Conversion Based on Urea Oxidation Reaction. *Small* **2020,** *16* (7), 1906133, DOI 10.1002/smll.201906133.

34. Ganiyu, S. O.; Martínez-Huitle, C. A.; Rodrigo, M. A., Renewable energies driven electrochemical wastewater/soil decontamination technologies: A critical review of fundamental concepts and applications. *Appl. Catal., B* **2020,** *270*, 118857, DOI 10.1016/j.apcatb.2020.118857.

35. Cao, Y.; Wang, K.; Wang, X.; Gu, Z.; Fan, Q.; Gibbons, W.; Hoefelmeyer, J. D.; Kharel, P. R.; Shrestha, M., Hierarchical porous activated carbon for supercapacitor derived from corn stalk core by potassium hydroxide activation. *Electrochim. Acta* **2016,** *212*, 839-847, DOI 10.1016/j.electacta.2016.07.069.

36. Yang, Y.; Chiang, K.; Burke, N., Porous carbon-supported catalysts for energy and environmental applications: A short review. *Catal. Today* **2011,** *178* (1), 197-205, DOI 10.1016/j.cattod.2011.08.028.

37. Tsai, W.; Yang, J.; Lai, C.; Cheng, Y.; Lin, C.; Yeh, C., Characterization and adsorption properties of eggshells and eggshell membrane. *Bioresour. Technol.* **2006,** *97* (3), 488-493, DOI 10.1016/j.biortech.2005.02.050.

38. Li, Z.; Zhang, L.; Amirkhiz, B. S.; Tan, X.; Xu, Z.; Wang, H.; Olsen, B. C.; Holt, C. M.; Mitlin, D., Carbonized chicken eggshell membranes with 3D architectures as high-performance electrode materials for supercapacitors. *Adv. Energy Mater.* **2012,** *2* (4), 431-437, DOI 10.1002/aenm.201100548.

39. Nasrollahzadeh, M.; Sajadi, S. M.; Hatamifard, A., Waste chicken eggshell as a natural valuable resource and environmentally benign support for biosynthesis of catalytically active Cu/eggshell, Fe_3O_4/eggshell and Cu/Fe_3O_4/eggshell nanocomposites. *Appl. Catal., B* **2016,** *191*, 209-227, DOI 10.1016/j.apcatb.2016.02.042.

40. Lu, S.; Hummel, M.; Gu, Z.; Gu, Y.; Cen, Z.; Wei, L.; Zhou, Y.; Zhang, C.; Yang, C., Trash to treasure: A novel chemical route to synthesis of NiO/C for hydrogen production. *Int. J. Hydrogen Energy* **2019,** *44* (31), 16144-16153, DOI 10.1016/j.ijhydene.2019.04.191.

41. Lu, S.; Gu, Z.; Hummel, M.; Zhou, Y.; Wang, K.; Xu, B. B.; Wang, Y.; Li, Y.; Qi, X.; Liu, X., Nickel Oxide Immobilized on the Carbonized Eggshell Membrane for Electrochemical Detection of Urea. *J. Electrochem. Soc.* **2020,** *167* (10), 106509, DOI 10.1149/1945-7111/ab9c80.

42. Maruthapandian, V.; Kumaraguru, S.; Mohan, S.; Saraswathy, V.; Muralidharan, S., An Insight on the Electrocatalytic Mechanistic Study of Pristine Ni MOF (BTC) in Alkaline Medium for Enhanced OER and UOR. *ChemElectroChem* **2018,** *5* (19), 2795-2807, DOI 10.1002/celc.201800802.

43. Ye, K.; Wang, G.; Cao, D.; Wang, G., Recent advances in the electro-oxidation of urea for direct urea fuel cell and urea electrolysis. *Top. Curr. Chem.* **2018,** *376* (6), 42, DOI 10.1007/s41061-018-0219-y.

44. Perdew, J. P.; Burke, K.; Ernzerhof, M., Generalized gradient approximation made simple. *Phys. Rev. Lett.* **1996,** *77* (18), 3865, DOI 10.1103/PhysRevLett.77.3865.

45. Kresse, G.; Hafner, J., Norm-conserving and ultrasoft pseudopotentials for first-row and transition elements. *J. Phys.: Condens. Matter* **1994,** *6* (40), 8245, DOI 10.1088/0953-8984/6/40/015.

46. Panchal, M.; Raghavendra, G.; Ojha, S.; Omprakash, M.; Acharya, S., A single step process to synthesize ordered porous carbon from coconut shells-eggshells biowaste. *Mater. Res. Express* **2019,** *6* (11), 115613, DOI 10.1088/2053-1591/ab4cb3.

47. Liu, H.; Wang, G.; Liu, J.; Qiao, S.; Ahn, H., Highly ordered mesoporous NiO anode material for lithium ion batteries with an excellent electrochemical performance. *J. Mater. Chem.* **2011,** *21* (9), 3046-3052, DOI 10.1039/C0JM03132A.

48. Zhai, Z.; Liu, Q.; Zhu, Y.; Cao, J.; Shi, S., Synthesis of $Ni(OH)_2$/graphene composite with enhanced electrochemical property by stirring solvothermal method. *J. Alloys Compd.* **2019,** *775*, 1316-1323, DOI 10.1016/j.jallcom.2018.10.262.

49. Aghazadeh, M.; Golikand, A. N.; Ghaemi, M., Synthesis, characterization, and electrochemical properties of ultrafine β-$Ni(OH)_2$ nanoparticles. *Int. J. Hydrogen Energy* **2011,** *36* (14), 8674-8679, DOI 10.1016/j.ijhydene.2011.03.144.

50. Su, Y.-Z.; Xiao, K.; Li, N.; Liu, Z.-Q.; Qiao, S.-Z., Amorphous Ni $(OH)_2$@three-dimensional Ni core–shell nanostructures for high capacitance pseudocapacitors and asymmetric supercapacitors. *J. Mater. Chem. A* **2014,** *2* (34), 13845-13853, DOI 10.1039/C4TA02486A.

51. Tong, Y.; Chen, P.; Zhang, M.; Zhou, T.; Zhang, L.; Chu, W.; Wu, C.; Xie, Y., Oxygen vacancies confined in nickel molybdenum oxide porous nanosheets for promoted electrocatalytic urea oxidation. *ACS Catal.* **2018,** *8* (1), 1-7, DOI 10.1021/acscatal.7b03177.

52. Daramola, D. A.; Singh, D.; Botte, G. G., Dissociation rates of urea in the presence of NiOOH catalyst: a DFT analysis. *J. Phys. Chem. A* **2010,** *114* (43), 11513-11521, DOI 10.1021/jp105159t.

53. Zhu, X.; Dou, X.; Dai, J.; An, X.; Guo, Y.; Zhang, L.; Tao, S.; Zhao, J.; Chu, W.; Zeng, X. C., Metallic nickel hydroxide nanosheets give superior electrocatalytic oxidation of urea for fuel cells. *Angew. Chem., Int. Ed.* **2016,** *55* (40), 12465-12469, DOI 10.1002/anie.201606313.

For Table of Contents Use Only

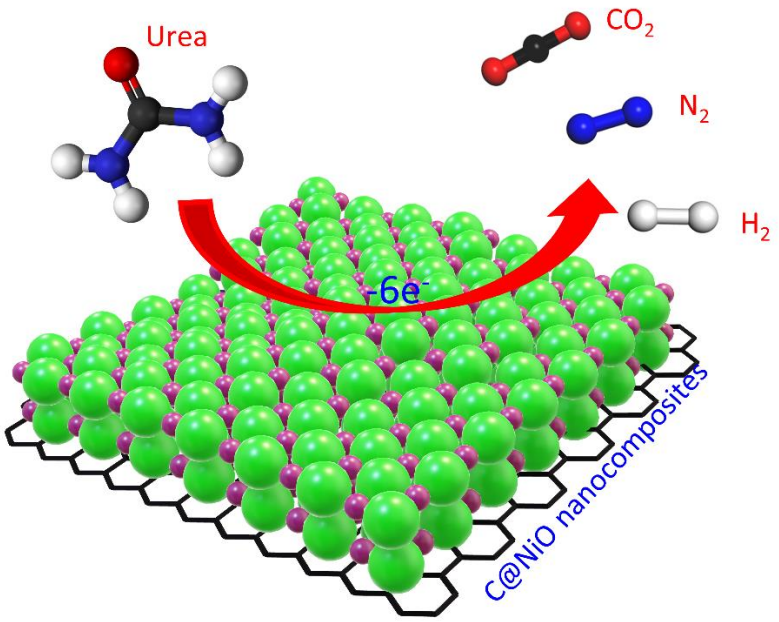

Synopsis

A strategy of using the biowaste eggshell membrane to produce the urea oxidation electrocatalyst was put forward.